doi: 10.5937/OTEH2402048I

Aerodynamic Optimization of Winglets for an Unmanned Aerial Vehicle

Dušan Ivković [1)]
Ivan Kostić [1)]
Olivera Kostić [1)]
Mirko Dinulović [1)]
Aleksandar Simonović [1)]

The main aim of this paper was to determine the influence of different parameters of winglet design on overall Unmanned Aerial Vehicle (UAV) aerodynamics. Looking from an aerodynamicist's point of view, the main reason for using such wingtip devices is to reduce induced drag component, which noticeably contributes to total drag when flying both in cruising flight and on higher angles of attack at lower speeds. Significant benefits of using winglets on overall aircraft performance include reduced fuel burn, increased maximum range and endurance, and higher cruise altitude.

Total drag of a simplified mock-up of an existing tactical UAV was calculated using hybrid approach. Parasite drag was obtained using analytical and semi empirical methods, while the induced drag and the lift in its linear domain were determined using inviscid CFD model based on a 3D vortex lattice method (VLM). Computational analyses were focused on determining the influence of winglet cant angle, root chord length, span, airfoil, and twist angle on lift-to-drag ratio of the UAV. Results obtained for different types of winglets (straight, blended and elliptical) were compared, and the best performing in the prescribed dimensions were the elliptical winglets. Their geometry was further optimized, finally providing an overall lift-to-drag ratio increase of 7% compared to the original UAV design without winglets, which represents quite remarkable improvement.

Key words: **Aerodynamics, Hybrid calculation method, UAV, VLM, Optimization of winglets, CFD.**

Motivation behind winglets

SINCE the Wright brothers first flew their "Wright Flyer" in 1903, the main goal of aeronautical engineers has been to make airplanes stay in the air the longest and fly the furthest distances possible. Today there are aircraft capable to circumnavigate entire Earth without refueling. Such an example is Virgin Atlantic's "Global Flyer" which in 2005. flew 36898 km in 67 hours, at an average speed of 550 km/h [1]. Difference in aerodynamic configurations between the Wright Flyer and the Global Flyer is obvious, and is best represented by comparing their maximum glide ratios, measuring 5.6 for the first [2], and 37 for the second [3].

Aerodynamic optimization became crucial in the last few decades because of the increasing jet fuel prices, and more and more rigorous ecological policies posted by the civil aviation authorities.

The use of wing tip devices in aviation is not a novelty. Inspiration for them came, like for a lot of other things in aviation, from birds. The first mention of winglet-like devices dates even before Wright brothers' first flight. English engineer Frederick W. Lanchester (1868.-1946.) patented wing end plates, aimed to reduce the influence of wingtip vortices, and they were based on different physical principles compared to modern day winglets. While the end plates were aimed to simply prevent the secondary wing tip flow (and to fully succeed in that, they would have to be extremely large), winglets use the secondary flow to generate a wing tip force with propulsive, forward oriented component. In the 1970's NASA scientists led by Richard Whitcomb worked on a scaled model of jet airplane, adding and optimizing for the first time the "real" winglets, which resulted in 9% [4] increase of lift to drag ratio. That is the moment airlines recognized benefits of adding winglets, starting to invest in their development, thus leading to their mass use. According to industry, since first introduced to fleets, NASA-developed winglets have saved airlines approximately 4 billion gallons of jet fuel [5].

Looking from an aerodynamicist point of view, main motivation behind all wingtip devices is reduction of induced drag, which, at moderate and high angles of attack most often generates very remarkable or even the major part of the overall drag.

Another potential reason for adding winglets can also be optimization of aircraft stability as shown in [6] for jet transport model, and in [7] for a tandem wing UAV, although this is definitely not their primary role.

Together with reducing costs of fuel burn, winglets contribute to the reduction of carbon dioxide emissions and also reduce the aircraft noise on takeoffs and landings.

Presented at the 11th International Scientific Conference on Defensive Technologies, Tara, Serbia, 9-11 October 2024.
1) University of Belgrade, Faculty of Mechanical Engineering, Kraljice Marije 16 Belgrade, SERBIA
Correspondence to: Dušan Ivković; e-mail: dudiivko@gmail.com

Characteristics of UAV

This paper is focused on determining the influence of different parameters of winglet design on the Pegasus Unmanned Aerial Vehicle (UAV) aerodynamic characteristics. For all here presented analyses only publicly available data were used, such as technical data available in [8] and 4 view drawing in [9]. All other data, such as the wing airfoil and its thickness ratio, were selected by the authors, based the available technical data and the intended UAV use.

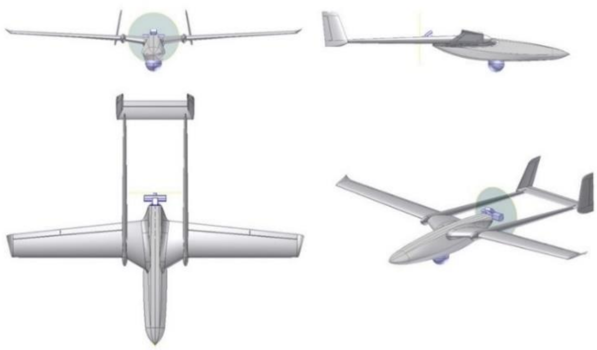

Figure 1. The UAV model [9]

Pegasus is a twin boom high wing UAV (Figure 1), with the following technical characteristics [8] and adopted airfoils:

Table 1. Characteristics of UAV model

Engine	2 stroke, horizontally opposed
Engine Power	32kw (43 hp)
Propeller	wooden, 2 blades
Wingspan	6.34 m
Wing Area	4.24 m^2
Length	5.395 m
Empty Weight	120 kg
Payload	40 kg
MTOW	230 kg
Max. speed	200 km/h
Cruise speed	130-150 km/h
Cruising altitude	3000 m
Endurance	12 h +
Here adopted wing airfoil	FX-67-K-170/17
Here adopted tail airfoil	NACA 0010

Hybrid method for drag coefficient estimation

Total drag was determined using hybrid approach, where parasite drag was determined using analytical and semi empirical methods, and induced drag was calculated using Vortex Lattice Method (VLM) software. Total drag formula can be written as [10]:

$$C_D = \underbrace{C_{Dmin} + k \cdot C_L^2}_{analytical+semi-empirical} + \underbrace{C_{Di}}_{VLM} \qquad (1)$$

First two members on the right side of (1) define the parasite drag, C_{Dmin} representing minimum drag coefficient of the entire UAV, and the second one $k \cdot C_L^2$ representing position component dependent on the angle of attack of the UAV. Third member C_{Di} represents lift induced drag component of total drag.

Parasite Drag Calculation

Parasite drag consists of form, friction and interference drag. Using analytical and semi empirical methods for estimating parasite drag in initial design phases provide good balance between accuracy and speed of calculation. In this paper parasite drag was determined using methods from [10, 11] which, combined with the VLM calculations for the induced drag, have proven to provide trustworthy results [12-15].

Calculated value of UAV's minimum drag coefficient without winglets is $C_{Dmin} = 0.0345$ [16]. Parameter k was determined using method from Douglas Aircraft Company [10] as $k = 0.38 \cdot C_{Dmin}$. Total drag equation (1) can now be written as:

$$C_D = 0.0345 + 0.013 \cdot C_L^2 + \underbrace{C_{Di}}_{VLM} \qquad (2)$$

Equation (2) represents total drag equation for UAV configuration without winglets, and was different for individual test cases, as a consequence of each winglet configuration having distinct parasite drag.

Induced Drag Calculation

Vortex lattice methods are used for 3D flow analyses over the lifting surfaces and entire aircraft configurations. They represent numerical methods based on inviscid CFD calculations and are mainly used in early stages of aircraft design. Software based on VLM are easy to use, provide fast solutions on modern computers, and even very complex geometries can be modelled relatively quickly, compared to more complex viscous CFD software packages. For all calculations presented in this paper, VLAERO+ software was used.

As explained in [17] in VLM airplane configuration is represented by multiple surfaces on which a grid of horseshoe vortices is superimposed. Velocities induced on control points by horseshoe vortices are calculated using Biot-Savart law. Then the summation is performed for all control points (on each element, e.g. the wing), which produces sets of linear algebraic equations for determining strength of each vortex. Solution must satisfy boundary conditions which state that flow through the element must be equal to zero. Strength of vortices is dependent on circulation over lifting surface, and difference of pressures on top and bottom of it. Difference of pressures is integrated in order to acquire forces and moments acting on aircraft.

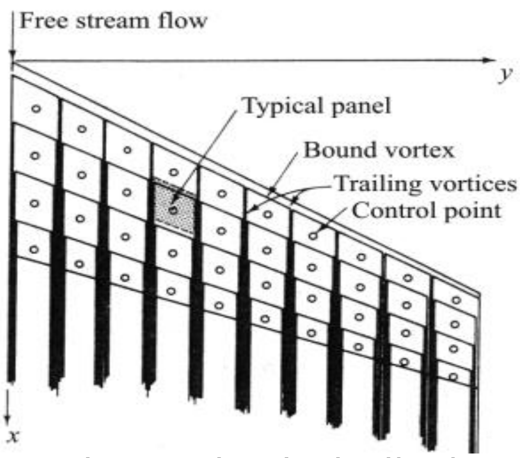

Figure 2. Coordinate system, elemental panels, and horseshoe vortices for a typical wing planform in the VLM [17].

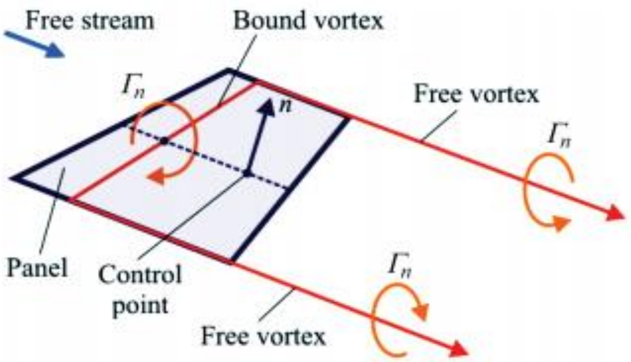

Figure 3. Representation of a single panel [14].

Horseshoe vortices are placed on trapezoidal panels. As shown in Figure 3, a horseshoe vortex consists of two semi-infinite free vortices and one bound vortex which coincides with the quarter-chord line of the panel, and is aligned with the local sweep angle. Control point is located on the three quarters chord position in the middle of the panel width.

Even though in VLM an airplane is formally represented by flat panels, this method accounts for the existence of airfoils, control surface deflections and fuselage cambers, by adding proper normals to each panel.

Vortex lattice methods can be used for the calculations of lift, moment and induced drag coefficients with remarkable precision considering their complexity. Since they are based on the potential flow model, obtained results are valid only in the domains of angles of attack and sideslip angles where separation effects are not immense.

Although performed analyses represent symmetrical flight cases, full model was created so further asymmetrical calculations can be performed in future. For VLM a relatively low number of panels is needed, only a single panel is required to predict the lift on a straight high-aspect ratio wing. Number of panels is chosen as to adequately define spanwise and chordwise lift distribution. In this particular case it was decided that adequate number of panels for the wing is 20 chordwise and 50 half-span wise, without winglets.

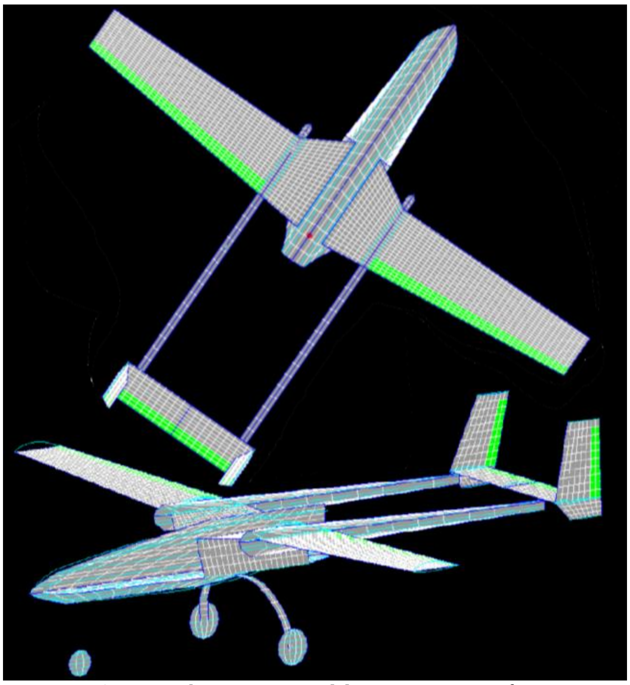

Figure 4. The UAV 3D model in VLAERO + software

Winglet design

The first stage in these analyses was to determine how different winglet design parameters influence the overall UAV aerodynamic characteristics. In order to quantify the benefits of different configurations, it was chosen to compare the UAV's maximum lift to drag $C_L\ f\ C_D$ ratios. All configurations were compared to UAV's lift to drag ratios without winglets, (Table 2). The influence of winglet cant angle, root chord length, span, airfoil, and twist angle on $C_L\ f\ C_D$ ratio of the UAV were calculated. Results obtained for different types of winglets (straight, blended and elliptical) were mutually compared, and the final winglet design was proposed and adopted.

Table 2. Characteristics of UAV without winglets

α[°]	C_L	C_{Dmin}	C_L^2	$k \cdot C_L^2$	C_{Di}	C_D	C_L/C_D
-6	-0.25	0.0345	0.062	0.00081	0.0239	0.0592	-4.196
-4	-0.06	0.0345	0.004	0.00005	0.0146	0.0492	-1.246
-2	0.13	0.0345	0.016	0.00021	0.0105	0.0452	2.781
0	0.31	0.0345	0.098	0.00128	0.0115	0.0473	6.613
2	0.50	0.0345	0.250	0.00327	0.0176	0.0554	9.022
4	0.69	0.0345	0.472	0.00619	0.0289	0.0696	9.877
6	0.87	0.0345	0.765	0.01003	0.0453	0.0898	9.737
8	1.06	0.0345	1.130	0.01482	0.0670	0.1163	9.140
10	1.25	0.0345	1.568	0.02056	0.0940	0.1491	8.400
12	1.44	0.0345	2.080	0.02726	0.1265	0.1882	7.661

Influence of Winglet Cant Angle, Chord Length, Winglet Span, Airfoil and Twist Angle

Initially, 13 straight winglets having the same span, chord length, taper ratio and airfoil were tested, with cant angle varying from 0 degrees (vertical, pointing upwards) to 180 degrees (vertical, pointing downwards) with 15 degrees steps (Figure 5). Obtained results are shown in Figure 6.

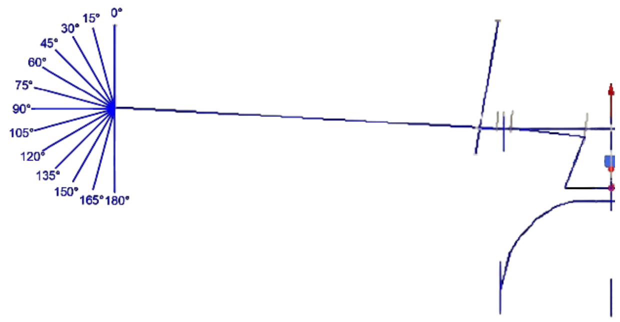

Figure 5. Tested variations of cant angle for straight winglets

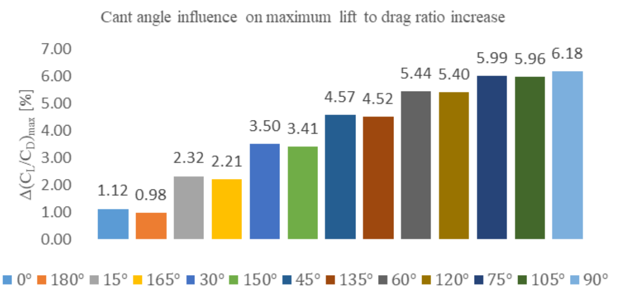

Figure 6. Cant angle influence on maximum lift to drag ratio increase (results shown in pairs symmetrical over horizontal axis).

Next the influence of winglet chord length was analyzed. For that purpose, three sets of straight winglets were designed, with same span and taper ratio, but with different chord lengths equal to 50%, 70% and 100% of wing tip chord, with cant angles varying from 0° to 90°, also with 15 degrees steps. Results are shown in Table 3.

Table 3. Results for winglets with different root chord lengths and same span

		0°	15°	30°	45°	60°	75°	90°
$\Delta\left(\frac{C_L}{C_D}\right)_{max}$ [%]	$0.5c_{tip}$	1.1	2.3	3.5	4.6	5.4	6.0	6.2
	$0.7c_{tip}$	1.5	2.9	4.3	5.6	6.6	7.2	7.4
	$1.0c_{tip}$	1.9	3.5	5.2	6.6	7.8	8.5	8.8

These winglets have different aerodynamic areas, which obviously influences their apparent contributions (increases with winglet area). So in the next phase, winglets with different chord sizes were tested but all having the same areas, achieved by keeping taper ratios the same, but adjusting the winglet spans. Results for cant angle of 30° are presented in Table 4.

Table 4. Results for winglets with different root chord lengths and same area

Cant angle 30°	$0.5c_{tip}$	$0.7c_{tip}$	$1c_{tip}$
$\Delta\left(\frac{C_L}{C_D}\right)_{max}$ [%]	3.5	3.47	3.11

Further analyses were focused on the influence of straight winglet's span on maximum $C_L\ f\ C_D$ ratio, and obtained results are graphically presented in Figure 7. They show that there is an obvious and progressive increase in maximum lift to drag ratio with the increase of winglet span, but this dependence is not linear, and for values above 1m it would be negligible.

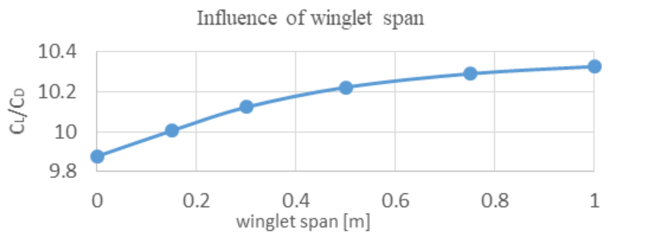

Figure 7. Influence of winglet span on UAV's maximum lift to drag ratio

Next the influence of the winglet airfoil was tested. Two sets of straight winglets were compared, with same geometries consisting of 30° cant angle, 50% wing tip chord length, 0.5m span and 0.4 taper ratio winglet, but with different airfoils, in first case having symmetrical NACA 0010 airfoil, and in second the asymmetrical FX-67K-170/17 [18, 19]. Results shown in Figure 8. show that having asymmetrical airfoil provides additional increase of maximum $C_L\ f\ C_D$ ratio.

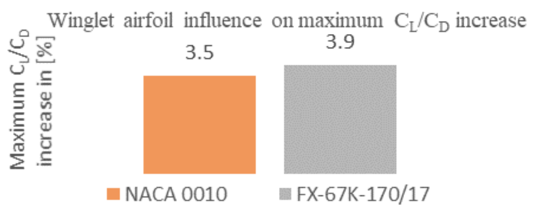

Figure 8. Influence of airfoil on maximum lift to drag ratio

The final winglet design parameter that was investigated was the twist angle. In this research, 7 different twist angles were analyzed on a straight winglet configuration described in the previous paragraph, showing relatively small influence of this parameter on maximum lift to drag ratio (Table 5).

Table 5. Influence of different twist angles on UAV's maximum lift to drag ratio

	Twist angle [°]						
	-3	-2	-1	0	1	2	3
$\left(\frac{C_L}{C_D}\right)_{max}$	10.195	10.205	10.214	10.223	10.231	10.238	10.245

From this chapter it was concluded that winglets symmetrical over horizontal axis provide similar benefits, thus in the following analyses only winglets pointing upwards were used, since they do not lower wings ground clearance. Root chord length initially seemed to have a big influence on increase of $C_L\ f\ C_D$ ratio when tested with same winglet span, but it was concluded that major contribution was indeed because of increased winglets surface area, which was proven in the next analysis where winglets areas were kept the same while different chord sizes were tested. Having in mind that in this scenario tested winglets have different spans, and that span also influences obtained results, and that it is very hard to compare just one parameter of winglets design while keeping others the same, influence of winglet span was tested showing increase of $C_L\ f\ C_D$ ratio, but only up to a certain length. Use of asymmetrical airfoil winglet provided better results versus symmetrical airfoil winglet, and it was concluded that twist angle can be used to fine tune final winglet design, providing small benefits.

Special Types of Winglets

In the previous chapter influence of the different parameters of the straight winglet design were tested. In the next stage three different winglet types were compared, in order to select the best for the final optimizations. All winglets were designed with the requirements not to exceed UAV's dimensions more than 30 cm horizontally from the wing tip, and more than 52 cm vertically from the wing tip, as shown in Figure 9. Requirements like this must be posted when designing winglets of a UAV that should be transported in predefined containers with strictly limited dimensions. The following winglet types were tested: two straight winglets, one designed to be the diagonal of a given rectangle and the other as a horizontal wing extension; two blended winglets, with different values of blending radius and cant angle, and the two elliptic winglets (Figures 9 and 10).

Blended winglets are designed with a radius blending the winglet with wing tip, and are designed with a smooth chord variation in the transition area where the wing joins the winglet minimizing vortex concentrations that produce drag.

Elliptic winglets are continuously curved from the joining point with the wing to its end tip, with curve representing the curvature of an ellipse, achieving minimum interference between wing and winglet. Same as with blended winglets they are designed with a smooth chord variation in the transition area where the wing joins the winglet to avoid vortex shedding from the leading edge.

Table 6. Different types of winglets

Winglet	$\Delta\left(\frac{C_L}{C_D}\right)_{max}$ [%]
Straight-diagonal	3.8
Straight-wing ext.	4.1

Blended 1	5.4
Blended 2	6
Elliptic 1	5.9
Elliptic 2	6.17

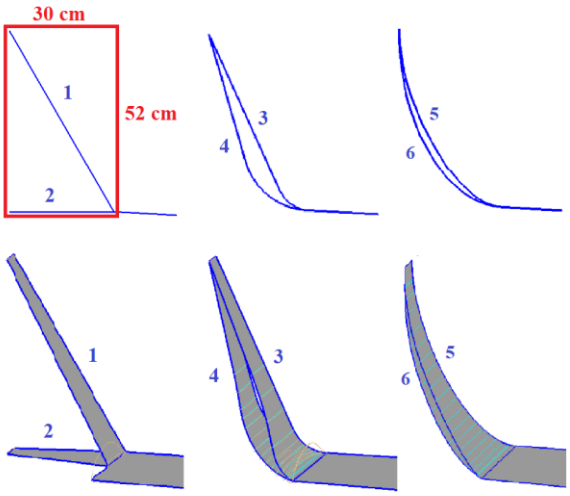

Figure 9. Winglet geometry limit box is marked red; 1 - straight diagonal type; 2 - straight horizontal wing extension type; 3 - blended 1 type; 4 - blended 2 type; 5 - elliptic 1 type; 6-elliptic 2 type

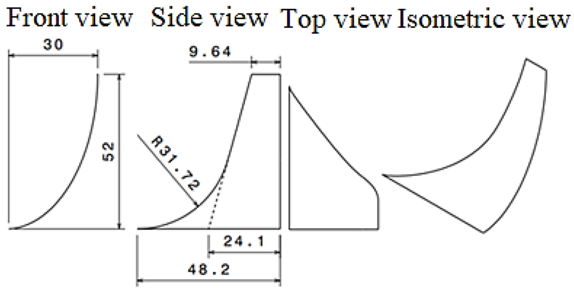

Figure 10. Elliptic 2 winglet type design parameters (all dimensions are in centimeters)

Initially all types of winglets were designed with no twist angle and symmetrical airfoil, in order to reduce number of test cases. From Table 6. it is obvious that the Elliptic 2 type winglet has given the best improvements in maximum lift to drag ratio, of 6.17%. Owing to that, it was selected for final optimizations. They were performed first by varying the twist angle, which provided best results when set at +3°, increasing UAV's maximum lift to drag ratio for additional 0.33%. Finally, changing the winglet airfoil from NACA0010 to FX-67K-170/17 has provided further increase of the maximum lift to drag ratio to 10.572, giving 7% increase when compared to original 9.877 of the initially analyzed UAV without winglets (Table 7.).

Table 7. UAV optimization results

Configuration of UAV	$\left(\frac{C_L}{C_D}\right)_{max}$	$\Delta\left(\frac{C_L}{C_D}\right)_{max}$ [%]
UAV without winglets	9.877	- - -
Elliptic 2 optimized winglets	10.572	7

Conclusion

In this paper different aspects of winglet design options were investigated, in order to evaluate their aerodynamic effectiveness and influence. For all calculations a hybrid approach was applied, where vortex lattice method was used to obtain the induced drag component for the entire UAV aerodynamic configurations, without and with the winglets. Parasite drag was calculated using analytical and semi empirical methods, and they were superimposed with induced drag obtained by VLM. Influence of winglet cant angle, chord length, span, airfoil, and twist angle was determined in order to better understand the influence of different design parameters and their combinations on overall UAV's aerodynamics. Additionally three different types of winglets were compared, with blended winglets showing better performance than straight winglets, and elliptic winglets outperforming both. Final winglet design was proposed, consisting of an optimized elliptic winglet, designed taking into consideration all results obtained during the research performed in this paper, increasing UAV's maximum lift to drag ratio by 7% . This methodology proved to be time efficient in providing valuable results when testing a vast number of different custom winglet designs.

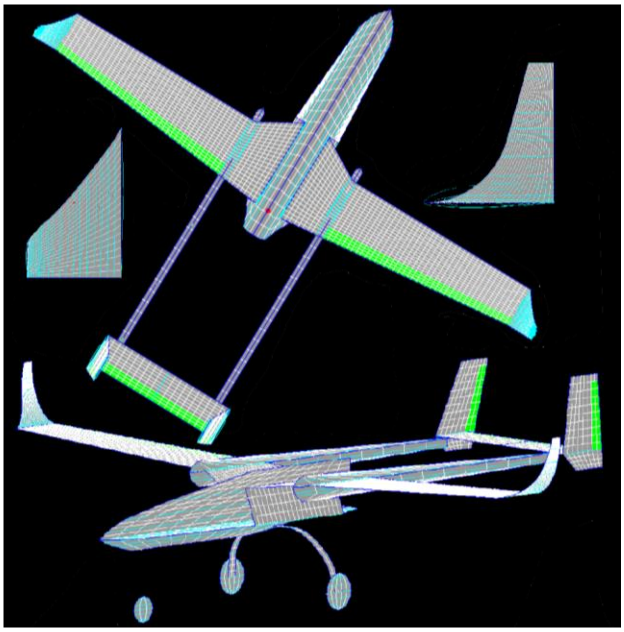

Figure 11. The UAV with Elliptic 2 optimized winglets

References

[1] World Air Sports Federation Records page, https://www.fai.org/records?f%5B0%5D=field_type_of_record%3A779, last accessed 2021/03/20

[2] ACKROYD,J.A.D.: Aerodynamics as the Basis of Aviation: How Well Did It Do?, Journal of Aeronautical History Paper No. 2018/01, 2018.

[3] NOLAND,D.: The Ultimate Solo, Popular Mechanics, vol. 180, no. 2, 74-79, 114-115, 2005.

[4] WHITCOMB,R.T.: A Design Approach and Selected Wind-Tunnel Results at High Subsonic Speeds for Wing-Tip Mounted Winglets, NASA TN D-8260, 1976.

[5] NASA article, https://www.nasa.gov/image-article/nasa-contribution-winglets/, last accessed 2024/01/22.

[6] JACOBS,P., Flechner,G.: The effect of winglets on the static aerodynamic stability characteristics of a representative second generation jet transport model, NASA TN D-8267, 1967.

[7] KOSTIĆ,I., SIMONOVIĆ, A., KOSTIĆ,O., IVKOVIĆ,D., TANOVIĆ,D.: Lateral-Directional Aerodynamic Optimization of a Tandem Wing UAV Using CFD Analyses, Aerospace, 11(3):223, 2024.

[8] VTI projects page, http://www.vti.mod.gov.rs/index.php?view=actuality&type=projects&category=1&id=138, last accessed 2024/01/22.

[9] VELIMIROVIĆ,K., VELIMIROVIĆ,N.: Tactical UAV Pegasus as a platform to carry missiles, In: Proceedings from 4th International Scientific Conference on Defensive Technologies OTEH 2011, 133-

136, 2011.

[10] SHEVELL,R.S.: Fundamentals of flight, Stanford University - Prentice-Hall International Editions, Englewood Cliffs, New Jersey, 1983.

[11] KOSTIĆ,I.: Applied Aerodynamics, handouts. University of Belgrade - Faculty of Mechanical Engineering, 2020.

[12] STEFANOVIĆ,Z., KOSTIĆ,I., KOSTIĆ,O.: Efficient Evaluation of Preliminary Aerodynamic Characteristics of Light Trainer Aircraft, Engineering Review, Vol. 32, 1, 49-56, 2012.

[13] STEFANOVIĆ,Z., KOSTIĆ,I., KOSTIĆ,O.: Primary Aerodynamic Analyses of a New Light Aircraft in Symmetrical Flight Configurations, Proceedings of the 7th International Symposium KOD 2012, 24-26.05.2012, Balatonfüred, Hungary, 97-104, 2012.

[14] STEFANOVIĆ,Z., KOSTIĆ,I., KOSTIĆ,O.: Hybrid Approach in the Initial Aerodynamic, Stability and Performance Calculations of a Light Aircraft, Technical Gazette, Vol. 20, 4, 605-614, 2013.

[15] KOSTIĆ,I., KOSTIĆ,O.: Several Approaches in Contemporary Light Aircraft Aerodynamic Design, Invited Presentation at The 3rd International Forum on Aerospace and Aeronautics AEROFORUM 2023, San Diego, USA, 2023.

[16] IVKOVIĆ,D.: Aerodinamička optimizacija vingleta za bespilotnu letelicu (Aerodynamic optimization of winglets for an Unmanned Aerial Vehicle), MSc Thesis, University of Belgrade, Faculty of Mechanical Engineering, Belgrade, 2021.

[17] BERTIN,J., CUMMINGS,R.: Aerodynamics for engineers, 5th Edition, Pearson Prentice - Hall, Upper Saddle River, NJ., 2008.

[18] STEFANOVIĆ,Z.: Airfoils (in Serbian), University of Belgrade, Faculty of Mechanical Engineering, Belgrade, 2005.

[19] LEDNICER,D.: The Incomplete Guide to Airfoil Usage, Aeromechanical Solutions LLC, Redmond, WA, https://m-selig.ae.illinois.edu/ads/aircraft.html, last accessed 2024/01/23.

Received: 01.07.2024.
Accepted: 10.09.2024.

Aerodinamička optimizacija vingleta za bespilotnu letelicu

Glavni cilj ovog rada je određivanje uticaja različitih parametara prilikom projektovanja vingleta na aerodinamičke karakteristike bespilotne letelice. Gledano iz perspektive aerodinamičara, glavni razlog za korišćenje vingleta je smanjenje indukovanog otpora, koji čini značajan deo ukupnog otpora prilikom krstarenja, kao i leta na većim napadnim uglovima pri manjim brzinama. Korišćenje ovakvih površina na krajevima krila doprinosi smanjenju potrošnje goriva, povećanju maksimalnog doleta i istrajnosti leta, kao i povećanju krstareće visine.

Ukupan otpor simulirane letelice, koja predstavlja približnu verziju postojeće taktičke bespilotne letelice je određen korišćenjem hibridnog pristupa. Parazitni otpor je određen analitičkim i poluempirijskim metodama, a indukovani otpor i uzgon u svom linearnom domenu su određeni korišćenjem neviskoznog CFD modela zasnovanog na 3D metodi vrtložne rešetke (VLM). Analize su fokusirane na određivanje uticaja nagibnog ugla vingleta, dužine tetive u korenu vingleta, razmaha vingleta, aeroprofila, i vitoperenja na finesu letelice. Upoređeni su i različiti tipovi vingleta (ravni, blendovani, i eliptični), a najbolje performanse u ispitivanim dimenzijama su ostvarili eliptični vingleti. Njihova geometrija je dalje optimizovana, čime je postignuto ukupno povećanje maksimalne finese od 7% u odnosu na osnovnu konfiguraciju bespilotne letelice bez vingleta, što predstavlja značajno poboljšanje.

Ključne reči: **Aerodinamika, Hibridna metoda, BPL, VLM, Optimizacija, CFD.**